

# Preparation of bioactive composite material for bone tissue repair

---

Šandrk, Nikolina

Master's thesis / Diplomski rad

2016

*Degree Grantor / Ustanova koja je dodijelila akademski / stručni stupanj:* **University of Zagreb, Faculty of Chemical Engineering and Technology / Sveučilište u Zagrebu, Fakultet kemijskog inženjerstva i tehnologije**

*Permanent link / Trajna poveznica:* <https://urn.nsk.hr/urn:nbn:hr:149:587254>

*Rights / Prava:* [In copyright](#)/[Zaštićeno autorskim pravom.](#)

*Download date / Datum preuzimanja:* **2024-06-28**



*Repository / Repozitorij:*

[Repository of Faculty of Chemical Engineering and Technology University of Zagreb](#)



UNIVERSITY OF ZAGREB  
FACULTY OF CHEMICAL ENGINEERING AND TECHNOLOGY  
GRADUATE STUDY

Nikolina Šandrk

# **MASTER THESIS**

Zagreb, September, 2016

UNIVERSITY OF ZAGREB  
FACULTY OF CHEMICAL ENGINEERING AND TECHNOLOGY  
GRADUATE STUDY

Nikolina Šandrk

PREPARATION OF BIOACTIVE COMPOSITE MATERIAL FOR BONE TISSUE REPAIR

MASTER THESIS

Mentor: prof. Marica Ivanković, PhD

Members of the Thesis Committee:

Professor Marica Ivanković, PhD

Anamarija Rogina, PhD

Hrvoje Ivanković, PhD

Zagreb, September, 2016

SVEUČILIŠTE U ZAGREBU  
FAKULTET KEMIJSKOG INŽENJERSTVA I TEHNOLOGIJE  
SVEUČILIŠNI DIPLOMSKI STUDIJ

Nikolina Šandrk

PRIPRAVA BIOAKTIVNOG KOMPOZITNOG MATERIJALA ZA POPRAVAK  
KOŠTANOG TKIVA

DIPLOMSKI RAD

Voditelj rada: prof. dr. sc. Marica Ivanković

Članovi ispitnog povjerenstva:

Prof. dr. sc. Marica Ivanković

Dr.sc. Anamarija Rogina

Prof. dr.sc. Hrvoje Ivanković

Zagreb, rujan 2016.

## ***Acknowledgements***

*The major part of the work described in this thesis was done in the Centre for Biomaterials and Tissue Engineering at the Polytechnic University of Valencia, Valencia, Spain, thanks to the Erasmus+ student mobility grant.*

*I would like to thank all the people who contributed in some way to this work.*

*First and foremost, I thank my supervisor, Professor Gloria Gallego Ferrer, for accepting me into her group, for continuous support and the valuable guidance throughout the work.*

*Furthermore, I would like to thank my mentor Professor Marica Ivanković for the expert guidance, advice and opportunities of making this master thesis.*

*Sincere thanks goes to Anamarija Rogina for introducing me to the topic as well for the helpful advice on the way. Her support and inspiring suggestions have been precious for the development of this thesis content; and to Laura Teruel Biosca for assistance with experimental part of the work.*

*I would like to express my gratitude to the committee members for the useful comments, remarks and engagement through the polishing of this master thesis.*

*I would also like to thank my roommate Chiara Collela for all the support and help. I will forever remember in my heart the stories and the moments you shared with me during these months together in Valencia.*

*Finally, I must express my very profound gratitude to my parents, sisters and to my friends for providing me with unfailing support and continuous encouragement throughout my years of study and through the process of researching and writing this thesis. This accomplishment would not have been possible without them.*

## **Zahvale**

*Većinski dio istraživanja proveden je u Centre for Biomaterials and Tissue Engineering, Polytechnic University of Valencia, Valencija, Španjolska, zahvaljujući Erasmus + programu.*

*Htjela bih se zahvaliti svim ljudima koji su na određen način pridonijeli izradi ovog rada.*

*Prvo i najvažnije hvala profesorici Gloriji Gallego Ferrer zbog mogućnosti izrade rada pod njezinim vodstvom te za konstantnu podršku i vrijedne smjernice za izradu ovog rada.*

*Nadalje zahvaljujem se svojoj mentorici prof.dr.sc Marici Ivanković na stručnom vodstvu i mogućnosti izrade diplomskog rada.*

*Iskreno i veliko hvala dr. sc. Anamariji Rogina za svu pomoć i savjete. Njena podrška i sugestije bili su ključni za izradu ovog rada. Zahvaljujem se i Lauri Teurel Biosca zbog pomoći pri eksperimentalnom dijelu rada.*

*Također moja zahvala članovima žirija za korisne komentare i primjedbe.*

*Hvala mojoj cimerici Chiari Collela za svu podršku i pomoć. Hvala za sve zajedničke trenutke provedene tijekom boravka u Valenciji.*

*Konačno, moja najveća zahvala odlazi mojim roditeljima, sestrama te prijateljima. Oni su mi pružali neograničenu podršku kroz ovih 5 godina studiranja. Bez njih ovo postignuće ne bi bilo moguće.*

## Summary

Tissue engineering and regenerative medicine has been providing exciting technologies for the development of functional macroporous biomaterials (scaffolds) aimed to repair and regenerate damaged bone. Biodegradability, high mechanical strength, osteointegration and formation of bony tissue are properties required for such materials. Bioactive synthetic hydrogels have emerged as promising materials because they can provide molecularly tailored biofunctions and adjustable mechanical properties, as well as an extracellular matrix-like microenvironment for cell growth and tissue formation.

In this study, injectable composite hydrogels were designed to be used in bone tissue regeneration. To mimic the mineralogical and organic components of the natural extracellular matrix of bone, hydroxyapatite and a tyramine conjugate of gelatin were combined to manufacture the composites. Gelatin conjugate is able to crosslink through the oxidative coupling of tyramine molecules, catalyzed by hydrogen peroxide and horseradish peroxidase, via non-cytotoxic conditions. The effect of various amounts of *in situ* synthesized hydroxyapatite in gelatin-tyramine solutions was investigated by analysing the morphology and physical properties of the resulting hydrogels. Characterization of hydroxyapatite within the hydrogels was performed by X-ray diffraction analysis and Fourier transform infrared spectroscopy. The morphology of prepared hydrogel was characterized using scanning electron microscope. Shear storage and loss moduli were measured as a function of gelation time, while the rheological properties of the completely crosslinked hydrogels were tested by changing the shear strain and frequency.

Results have confirmed adequate formation of apatite within the gelatin-tyramine matrix. Microscopy reveals better dispersion of hydroxyapatite crystals by *in situ* synthesis than in control samples prepared by classical blending. The rheological testing has shown no significant effect of hydroxyapatite content on the gelation time with respect to pure gelatin-tyramine matrix, while shear strength of the different hydrogels seems to need to be further investigated.

Keywords: injectable hydrogels, *in situ* hydroxyapatite, gelatin-tyramine, gelation time, rheology.

## ***Priprava bioaktivnog kompozitnog materijala za popravak koštanog tkiva***

### **Sažetak**

Inženjerstvo tkiva i regenerativna medicina pružaju mnoge razvijene tehnologije za razvoj funkcionalnih nadomjestaka, kojima je cilj popravak ili regeneracija koštanog tkiva ili organa. Karakteristike koje takvi materijali trebaju ispunjavati su biorazgradivost, visoka mehanička čvrstoća, osteointegracija i stvaranje koštanog tkiva. Kao obećavajući materijali javili su se bioaktivni, sintetski hidrogelovi zbog mogućeg pružanja molekularno prilagođenih biofunkcija, podesivih mehaničkih svojstava te pogodni mikrokoliš za razvoj stanica i stvaranje tkiva.

U ovom radu, pripremljeni su kompozitni hidrogelovi za popravak koštanog tkiva. Za imitaciju kemijskog sastava prirodne kosti, kao komponente su se koristili hidroksiapatit i želatina modificirana tiraminom. Stvaranje injekcijskih hidrogelova postignuto je djelovanjem enzima peroksidase uz pomoć vodikova peroksida. Istraživan je utjecaj različite koncentracije *in situ* sintetiziranog hidroksiapatita istraživan je na morfologiji i fizikalnim svojstvima hidrogela. Prisutnost hidroksiapatita u hidrogelovima potvrđena je karakterizacijskim tehnikama uključujući rendgensku difrakcijsku analizu i infracrvenu spektroskopiju s Fourierovim transformacijama. Morfologija pripremljenih hidrogelova istražena je pretražnim elektronskim mikroskopom. Smični modul pohrane i gubitka mjereni su u ovisnosti o vremenu geliranja, dok su reološka svojstva potpuno umreženog gela ispitana promjenom smične deformacije i frekvencije.

Rezultati karakterizacije potvrdili su stvaranje apatitne faze unutar matrice modificirane želatine. Mikroskopska analiza ukazuje na bolju disperziju hidroksiapatita sintetiziranog *in situ* u odnosu na kontrolne uzorke dobivene klasičnim umiješavanjem. Reološka ispitivanja pokazala su da ne postoji utjecaj različitog udjela hidroksiapatita na vrijeme geliranja u odnosu na tiraminom modificiranu želatinu, dok se utjecaj reoloških parametara na smičnu čvrstoću različitih hidrogelova treba detaljnije istražiti.

Ključne riječi: injekcijski hidrogelovi, *in situ* hidroksiapatit, tiraminom modificirana želatina, vrijeme geliranja, reologija.



# ***Content***

1. Introduction.....	1
2. State of the art .....	4
2.1. Hydrogels .....	4
2.2. Injectable hydrogels .....	6
2.2.1. Injectable gelatin-based hydrogels .....	8
2.2.2. In situ precipitation of hydroxyapatite.....	9
2.4. Materials and methods .....	13
2.4.1. Materials .....	13
2.4.2. Tyramine grafting to gelatin .....	13
2.4.3. Synthesis of hydroxyapatite particles as a control material .....	14
2.4.4. In situ synthesis of composite hydrogels.....	14
2.4.5. Injectable composite hydrogel preparation.....	15
2.5. Materials characterization .....	15
2.5.1. The pH monitoring .....	15
2.5.2. Fourier transform infrared spectroscopy .....	15
2.5.3. X-ray diffraction analysis .....	16
2.5.4. Scanning electron microscopy.....	16
2.5.5. Equilibrium swelling .....	16
2.6. Rheological properties.....	17

3. Results and discussion .....	18
3.1. FTIR identification.....	18
3.2. Determination of mineralogical composition.....	21
3.3. Microstructure of injectable hydrogels .....	24
3.4. Equilibrium water swelling of crosslinked hydrogels.....	27
3.5. Rheological properties of hydrogels .....	28
3.5.1. Determination of gelation time.....	28
3.5.2. Shear strength of crosslinked composite hydrogels .....	29
4. Conclusions.....	33
5. Literature.....	34

## ***1. Introduction***

A variety of bioactive organic-inorganic composites have been investigated over the last two decades as scaffolds for pathological or damaged bone in the human body. Bioactive organic-inorganic composites are materials formed by an organic matrix and a reinforcement of inorganic particles. Those kinds of materials are inspired on the composition of the living bone and the particles usually provide matrix strengthening and bioactivity. At the ultra-structural level, human bone is a composite material consisted of nanometric apatite crystals and collagen fibres, therefore a polymer matrix composite containing a bioactive component as a particulate appears a natural choice for a bone substitute. The bioactivity of the composite, which is rendered by the bioactive component in the composite, promotes the tissue growth adjacent to the implant and the formation of a strong bond between the tissue and the implant after implantation [1,2]. As such, bioactive composite materials have an important role in the development of bone tissue engineering. There are multiple clinical reasons to develop bone tissue-engineered alternatives, including the necessity for better filler materials that can be used in the reconstruction of large orthopaedic defects and for orthopaedic implants that are mechanically more suitable for biological environment.

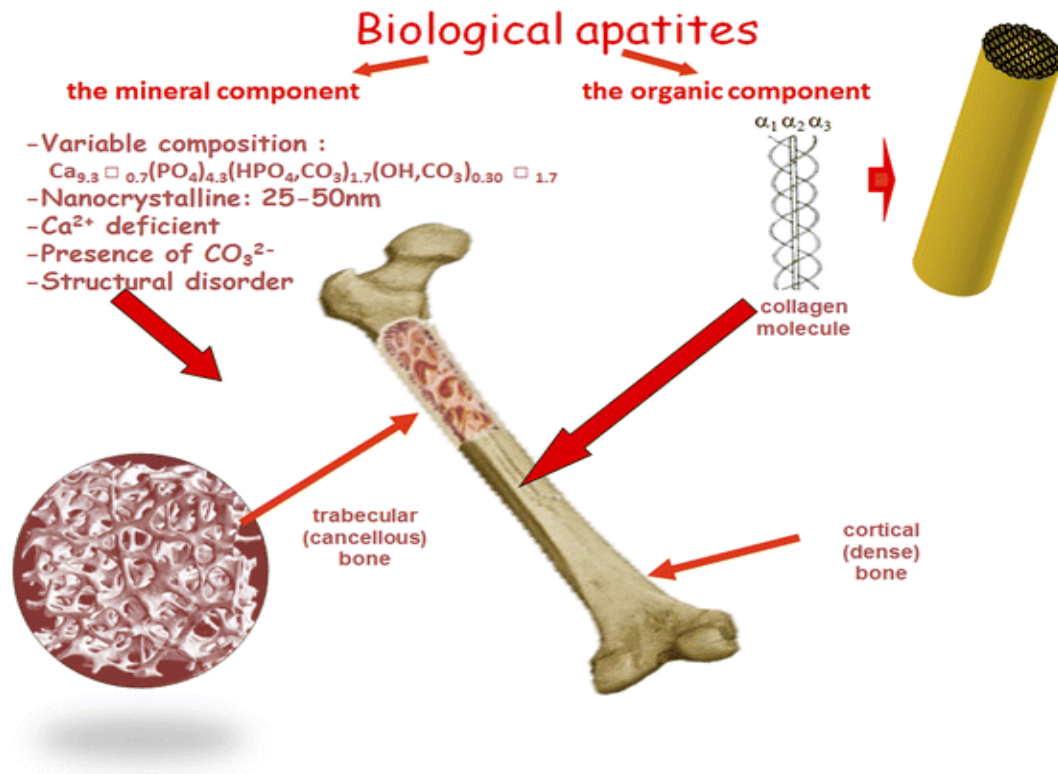


Figure 1. Hierarchical bone structure at various scales [3].

Bone tissue engineering (BTE) is based on the understanding of bone structure (Figure 1), bone mechanics, and tissue formation as it aims to induce new functional bone tissues. The classic BTE paradigm highlights several key players: a) a biocompatible scaffold that closely mimics the natural bone extracellular matrix niche, b) osteogenic cells to deposit the bone tissue matrix, c) morphogenic signals that help to direct the cells to the phenotypically desirable type, and d) sufficient vascularization to meet the growing tissue nutrient supply and clearance needs [4].

Among tissue reconstruction strategies, the use of biomaterials is an attractive alternative method due to their flexibility and possibility for further development. In addition to providing a broad range of materials, biomaterials allow for structural manipulations to improve the dispositive biocompatibility and increase the chance of success in reparative and regenerative procedures [5].

The evolution of bone graft biomaterials can be categorized into four different generations. The first generation of bone grafts are metals and alloys which have excellent

mechanical properties, but are neither bioresorbable nor bioactive. Their lifetime is limited and hence need to be removed and replaced surgically. The second generation of bone grafts includes bioactive ceramics and bioresorbable polymers. The third generation of bone grafts is focused on composite scaffolds which combine the strength, stiffness and osteoconductivity of ceramics with the flexibility, toughness and resorbability of polymers. Fourth generation of bone grafts are polymer-ceramic composite scaffolds with the incorporation of osteogenic cells, growth factors or bone morphogenetic proteins, used alone or in a combination [6].

One of the greatest advances in bone tissue engineering has also been a development of hydrogels, which present properties suitable for biomedical application. Structurally, these systems resemble the extracellular matrix of many natural tissues, giving them high biocompatibility. In addition, hydrogels have flexible processing methods and can be used as scaffolds, controlled release systems for drugs, cells or growth factors, and as barriers or adhesives at the biomaterial-tissue interface. Recently, hydrogels that exhibit *in situ* gelation have been widely researched due to their ability to remain liquid at room temperature and become gel at body temperature which makes them suitable for injection purposes. Therefore, injectable hydrogels, which offer minimally invasive surgery are promising scaffolds for cell encapsulation, drug delivery, tissue repair, and reconstructive surgery. Nonetheless, injectable hydrogels may be well suited to tissue repair, but they have to be biocompatible, biologically stable, and without toxic initiating system [7]. Moreover, they can fill even small and irregular damaged cavities, easily incorporate therapeutic agents, and be manipulated to improve their physical and bioactive properties [5].

## ***2. State of the art***

### ***2.1. Hydrogels***

Over the years, researchers have defined hydrogels in many different ways. The most common proposition is that hydrogel is a water-swollen cross-linked polymer network produced by the simple reaction of one or more monomers [8]. Another definition is that a polymer material exhibits the ability to swell and retain a significant fraction of water within its structure, but will not dissolve in water. Hydrogels have received considerable attention in the past 50 years due to their exceptional promise in wide range of applications. They possess also a degree of flexibility very similar to natural tissue due to their large water content [9].

Natural origin hydrogels have gained much popularity because of their similarity to the extracellular matrix (ECM) and higher regeneration rate [10]. They are widely recognized as a useful material for a wide range of biopharmaceutical and biomedical applications due to their excellent properties, such as high biocompatibility and low mechanical irritation of surrounding tissues after implantation *in vivo*. Hydrogel's network can be prepared from natural, synthetic polymers or polymer blends and hybrids. Based on the polymer origin, hydrogels can be classified into three major types: 1) natural, 2) synthetic, and 3) synthetic-natural hybrid hydrogels.

This section describes the properties of polymers that have been used for designing and fabricating the hydrogel scaffolds. The mostly used polymers for mentioned purpose are natural polymers. Natural polymers have been used to make natural hydrogels as scaffolds for tissue engineering owing to their biocompatibility, inherent biodegradability and critical biological functions. There are four major types of natural polymers, including:

- 1) *Proteins*, such as collagen, gelatin, fibrin, silk;
- 2) *Polysaccharides*, such as hyaluronic acid, agarose, dextran and chitosan;
- 3) *Protein/polysaccharide hybrid polymers*, such as collagen/hyaluronic acid, laminin/cellulose, gelatin/chitosan and fibrin/alginate;
- 4) *DNA* [11-13].

However, the application of natural hydrogels is often restricted because of concerns regarding potential immunogenic reactions and relatively poor mechanical properties.

Compared with natural polymers, synthetic polymers possess more reproducible physical and chemical properties, which is critical for the fabrication of tissue-engineered scaffolds. Currently, synthetic polymers have emerged as an important alternative for fabricating hydrogel tissue-engineered scaffolds because they can be molecularly tailored with block structures, molecular weights, mechanical strength and biodegradability. Synthetic polymers used for preparing synthetic hydrogels are classified into three major types, including non-biodegradable, biodegradable and bioactive polymers. Biodegradability is one of the most important considerations of scaffolds for tissue engineering. It is highly desirable to ensure that the biodegradation rate coincides with new tissue regeneration at the defect site [14].

Hydrogels are broadly classified into two categories:

1. Permanent/chemical gel: they are called 'permanent' or 'chemical' gels when they are covalently cross-linked networks. Therefore, they are stable and cannot be dissolved in any solvents unless the covalent crosslink points are cleaved.
2. Reversible/physical gel: they are called 'reversible' or 'physical' gels when the networks are held together by molecular entanglements, and/or secondary forces including ionic, hydrogen bonding or hydrophobic interactions. In physically cross-linked gels, dissolution is prevented by physical interactions, which exist between different polymer chains. All of these interactions are reversible, and can be disrupted by changes in physical conditions or application of stress.

Although physically crosslinked hydrogels have the general advantages of forming gels without the need for chemical modification or the addition of crosslinking entities, they have some limitations. It is difficult to decouple variables such as gelation time, network pore size, chemical functionalization, and degradation time; this restricts the design flexibility of a physically crosslinked hydrogel because its strength is directly related to the chemical properties of the constituent gelling agents. In contrast, chemical crosslinking results in a network with a relatively high mechanical strength and, depending on the nature of the chemical bonds in the building blocks and the crosslinks, relatively long degradation times. Chemically crosslinked

gels are also mechanically stable owing to the covalent bond in these gels. The detailed classification is presented in table 1 [15].

Table 1. Methods for synthesizing physically and chemically crosslinked hydrogels.

Physically crosslinked hydrogels	Chemically crosslinked hydrogels
Ionic interactions (alginate etc.)	Polymerization (acryloyl group etc.)
Hydrophobic interactions (PEO–PPO–PEO etc.)	Radiation ( $\gamma$ -ray etc.)
Hydrogen bonding interactions (PAAc etc.)	Small-molecule crosslinking (glutaraldehyde etc.)
Stereocomplexation (enantiomeric lactic acid etc.)	Polymer–polymer crosslinking (condensation reaction etc.)
Supramolecular chemistry (inclusion complex etc.)	

## 2.2. Injectable hydrogels

A major achievement of hydrogel-based technology is the development of *in situ* crosslinking mechanisms which renders the system injectable by allowing an aqueous mixture of gel precursors and bioactive agents to be administered using a syringe [16]. In particular, *in situ* gelling hydrogels have attracted attention for drug delivery application and tissue regeneration [17]. Compared with preformed hydrogels, *in situ* gelling hydrogels are attractive because they can fill any shape of a defect, allow homogeneous incorporation of therapeutic molecules or cells, and do not require surgical procedures for implantation [18].

*In situ* gelling hydrogels can also be subdivided into the two categories above mentioned: 1) *chemical crosslinking* (such as photocrosslinking, Michael-type reactions, Schiff-base formation reactions), and 2) *physical crosslinking* (such as ionic interactions, hydrophobic interactions and stereocomplexation) [19-21].



Physically crosslinked hydrogels are usually formed under mild conditions providing a friendly environment to cells and bioactive molecules. However, they generally have a low mechanical strength, and changes in the external environment (e.g. ionic strength, pH, temperature) may give rise to disruption of the hydrogel network. Chemically crosslinked hydrogels, on the other hand, may exhibit enhanced mechanical strength and better stability, but with possible lower bioactivity and biocompatibility. In order to obtain a chemically crosslinked hydrogel, the use of additives such as photo-initiators, crosslinking agents, or organic solvents are often required [22]. Those additives may be cytotoxic, resulting in a non-biocompatible hydrogel. Photocrosslinking as one of the methods for injectables may also lead to a local increase of temperature, which subsequently may damage neighbouring cells and tissues.

An emerging approach for *in situ* formation of hydrogels is based on enzyme-catalyzed crosslinking reactions. Usually, hydrogels have been obtained by horseradish peroxidase (HRP)-catalyzed crosslinking reactions [23]. HRP is a single-chain  $\beta$ -type hemoprotein that catalyzes the coupling of phenol or aniline derivatives via decomposition of hydrogen peroxide [24]. As a natural polymer possessing functional groups, gelatin has a potential to form HRP-catalyzed injectable hydrogels for cell encapsulation. However, the lack of HRP-reactive groups requires additional modification of gelatin macromolecules.

### ***2.2.1. Injectable gelatin-based hydrogels***

Gelatin is a natural polymer composed of amino acids. It is produced by partial hydrolysis of collagen extracted from the skin, bones and connective tissues of domestic animals [25]. It is commonly used for pharmaceutical and medical applications due to its biodegradability and biocompatibility in physiological environments. The chemical properties of gelatin are affected by amino acid composition, which is similar to that of the parent collagen, thus influenced by animal's species and type of tissues [26]. In the present work, we used porcine skin gelatin which is produced from acidic treatment and it is known as the type A gelatin.

Aqueous gelatin solution, obtained by heating a suspension of gelatin powder to over approximately 40 °C will form physical hydrogels when cooled down to less than 30 °C. Gelatin forms a triple helix in a solid state, however, upon heating in water some of its triple helices dissolve forming a gel after cooling. This is because the triple helice structures act as crosslinking points of the hydrogel. If subsequently heated to around 40 °C, the  $\alpha$ -helices remelt and result in a gel-to-sol transition. This means that, at a body temperature, gelatin is in liquid state and cannot form a stable hydrogel limiting the application of thermally-induced formation of gelatin hydrogels in tissue engineering.

To avoid dissolution, lot of studies include the application of chemical crosslinker as glutaraldehyde, genipin, carbodiimides etc. A drawback of those crosslinkers is the potentially cytotoxic chemical reactions to form the hydrogel, which has to be performed outside of the body. Several washes are necessary to remove residual and unreacted products after gelation. Besides, the obtained hydrogel has the shape of the mould in which it was produced.

Recently, gelatin-tyramine conjugates have been proposed as injectable hydrogels as they form stable hydrogels under a non-cytotoxic enzymatically catalyzed reaction in the presence of small amounts of hydrogen peroxide. Gelatin derivatives possessing phenol groups were synthesized by combining gelatin and tyramine hydrochloride via the carbodiimide-mediated condensation of the carboxyl groups of gelatin and the amino groups of tyramine, as shown in figure 2 [21]. Controlling the content of phenol groups can tune the mechanical properties of gelatin hydrogels. It has been found that the resistance forces increase by decreasing the content of phenol groups [18].

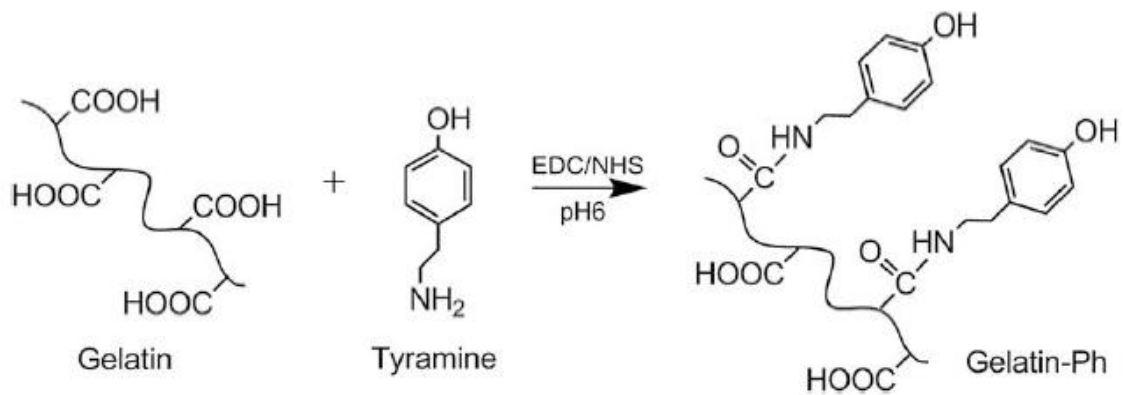


Figure 2. Synthesis scheme of gelatin–phenol (gelatin-Ph) derivative using tyramine [28].

### 2.2.2. *In situ precipitation of hydroxyapatite*

Numerous studies on apatite and polymer-apatite composites have confirmed positive influence of hydroxyapatite on cell proliferation, differentiation and growth *in vitro* and *in vivo* [27-29]. Therefore, incorporation of hydroxyapatite within gelatin matrix can mimic a complex composition of natural bone which is mainly composed of a mineralized organic phase, i.e. collagen fibres with nanometric crystals of calcium phosphate (apatites). Hydroxyapatite and other related calcium phosphate minerals have been utilized extensively as implant materials for many years due to their excellent biocompatibility and bone bonding ability, and structural and compositional similarity to the mineral phase of hard tissue [30].

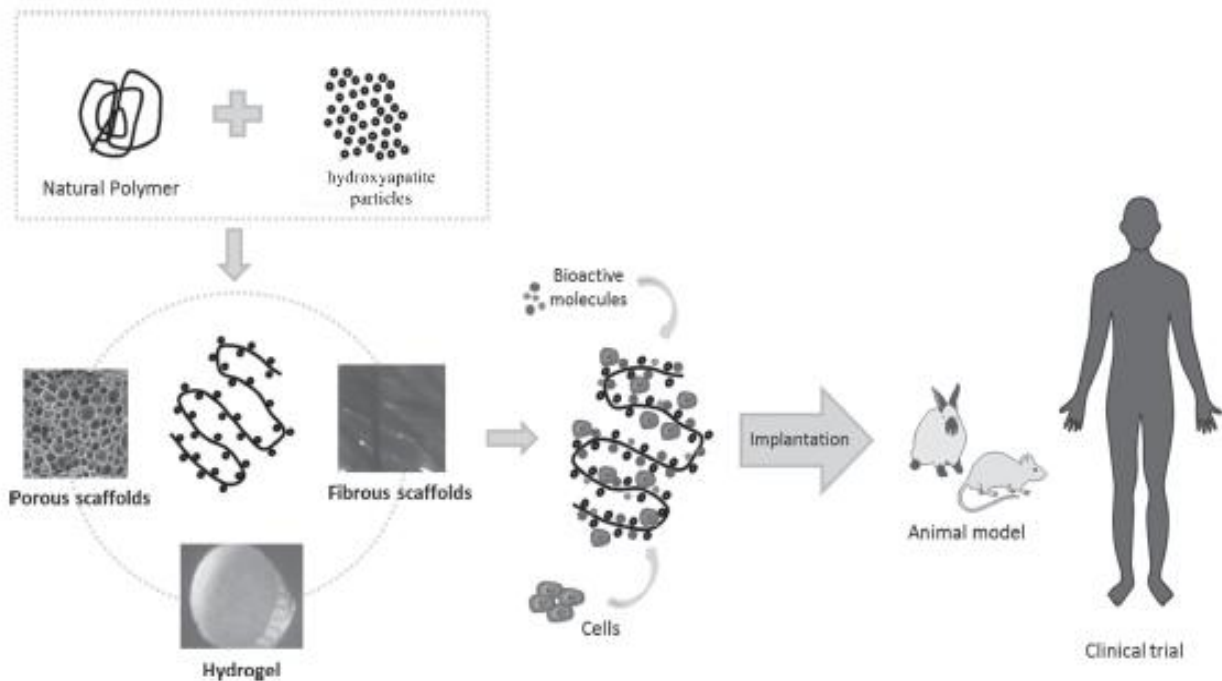


Figure 3. Tissue engineering strategy of biopolymer/calcium phosphate nanocomposites [4].

Hydroxyapatite (HA) with the chemical formula  $\text{Ca}_{10}(\text{PO}_4)_6(\text{OH})_2$  is one of the calcium phosphate (CaP) ceramics and it is clinically available as a synthetic bone substitutes [31]. Hydroxyapatite's excellent properties of bioactivity, osteoinductivity and osteoconductivity lie on its biologically resorbable nature and ability for ionic substitution.

Hydroxyapatite is chemically similar to bone mineral but it lacks many other ions that are also present in native bone. Substitutions can be made into the hydroxyapatite lattice to mimic the chemical composition of bone more closely. The first type of substitution is a cationic substitution where the substituted ions replace the calcium atoms in the lattice. The other type, anionic, has two forms as it covers substitutions for the both the hydroxyl (type A) and phosphate (type B) groups.

A potential method of producing synthetic HA with enhanced osteointegration is to incorporate ions that are present in bone mineral, such as carbonate ions, into the HA structure. In addition to calcium, phosphate and hydroxyl ions, the inorganic component of hard tissues contains a significant proportion of carbonate ions (2 – 8 wt.%). Carbonate ion substitution has

the effect of inducing lower crystallinity and a higher number of structural defects within the HA structure [32].

Hydroxyapatite can be prepared either as stoichiometric HA or as calcium-deficient HA. Stoichiometric apatite,  $\text{Ca}_{10}(\text{PO}_4)_6(\text{OH})_2$ , has a Ca/P ratio of 10:6, normally expressed as 1.67. It is used in various medical applications such as repairing of bone defects and bone augmentation, orthopaedics, odontology, coating of metal implants etc. In contrast to stoichiometric calcium HA with a Ca/P molar ratio of 1.67, biological apatites contain minor substituent in their structure ( $\text{CO}_3^{2-}$ ,  $\text{Cl}^-$ ,  $\text{Mg}^{2+}$ ,  $\text{K}^+$ ,  $\text{Na}^+$ ). Those types of apatites are usually calcium-deficient with a Ca/P molar ratio lower than 1.67, and  $\text{CO}_3^{2-}$  substitutes primarily for  $\text{PO}_4^{3-}$  groups (B-type substitution) [33].

Hydroxyapatite can be synthesised via numerous production routes in wet state (precipitation, hydrothermal technique, hydrolysis of other calcium phosphates), using a range of different reactants. Depending upon the technique, materials with various morphology, stoichiometry, and level of crystallinity can be obtained. Wet-chemical precipitation route is the most talented route owing to its ease in experiment operations, low working temperature, high percentages of pure products and inexpensive equipment requirement [34]. Usually, precipitation method is based on the addition one precursor to another in a stoichiometric ratio of calcium and phosphorus (Ca/P = 1.67) with continuous stirring and pH regulation [35]. The most common hydroxyapatite synthesis is based on reaction of calcium and orthophosphate ions originated from different starting materials.

Up till now, researches of hydrogels based on gelatin and hydroxyapatite have been conducted. Peng and Wang have synthesized a composite of gelatin and hydroxyapatite using glutaraldehyde as a crosslinker [36]. Azami and Rabie have been designed glutaraldehyde crosslinked gelatin/hydroxyapatite nanocomposite as well [24]. According to the available literature, synthesis of injectable composite hydrogel based on *in situ* formed hydroxyapatite and tyramine grafted gelatin has not yet been proposed.

The synthesis of polymer-apatite hydrogels simply by blending both phases can rise up difficulties in the homogeneity of the microstructure of the final product. To minimize the agglomerating factor of hydroxyapatite particles added into the matrix, the *in situ* synthesis has been proposed. Usually, nitrate precursors as a source of calcium ions have been used regardless to the possibility of development of toxic nitrogen oxides (NO<sub>x</sub>). As previously stated, biological apatite is carbonate-substituted hydroxyapatite. Thus, calcium carbonate as a non-toxic calcium precursor could provide *in situ* synthesis of biologically more active apatite phase similar to biological one. The formation of hydroxyapatite crystals *in situ* from initial calcium carbonate can be accomplished by using urea phosphate as a simultaneous phosphate precursor and pH regulator by thermal degradation of urea during the HA synthesis. Finally, it is assumed that specific groups of gelatin macromolecules (-COOH) could provide ordered structure of *in situ* synthesized hydroxyapatite by acting as nucleation sites for apatite crystallization.

## **2.4. Materials and methods**

### **2.4.1. Materials**

Chemicals used for the preparation of injectable composite hydrogels are listed below:

- Gelatin from porcine skin (powder, gel strength ~300 g Bloom, type A; Sigma-Aldrich USA)
- Tyramine hydrochloride (C<sub>8</sub>H<sub>12</sub>ClNO; Sigma-Aldrich, USA)
- Calcium carbonate (CaCO<sub>3</sub>, calcite; TTT, Croatia)
- Urea phosphate (UPH, (NH<sub>2</sub>)<sub>2</sub>CO-H<sub>3</sub>PO<sub>4</sub>; Aldrich Chemistry, USA)
- Horseradish peroxidase (HRP, type VI, 298 purpurogallin unit/mg solid was purchased from Aldrich and used without further purification)
- Hydrogen peroxide solution (H<sub>2</sub>O<sub>2</sub>, 30% (w/w) in H<sub>2</sub>O, contains stabilizer; Aldrich Chemistry, USA)

The preparation of investigated materials can be divided into several steps: 1) synthesis of polymer matrix (gelatin-tyramine); 2) synthesis of control material (hydroxyapatite particles); 3) *in situ* synthesis of composite hydrogels, 4) synthesis of injectable composite hydrogels.

### **2.4.2. Tyramine grafting to gelatin**

The modified gelatin to be later used as an injectable hydrogel was obtained by grafting the amine groups of tyramine to the carboxylic groups of gelatin. The molar ratios for the grafting were tyramine/*N*-(3-dimethylaminopropyl)-*N'*-ethylcarbodiimide hydrochloride (EDC)/COOH = 2/2/1 and *N*-hydroxysuccinimide (NHS)/EDC = 1/10. Briefly, 3% (w/v) gelatin was dissolved in 50 mmol/dm<sup>3</sup> 2-(*N*-morpholino)ethanesulfonic acid (MES) at 60 °C for 30 min under stirring (0.6 g of gelatin and 0.195 g of MES in 20 mL).

Then 0.111 g of tyramine hydrochloride was added and the mixture was stirred for 20 min at room temperature. The pH was adjusted to 6, and 7 mg of NHS was added and stirred for 30 min

for homogenization. Afterwards, 123 mg of EDC was added to the mixture and stirred for another 24 h at 37 °C. Unreacted reagents were removed via dialysis against deionized water for 48 h. Finally, the modified gelatin was lyophilized for further use and denoted as 'gel-tyr'.

### ***2.4.3. Synthesis of hydroxyapatite particles as a control material***

Hydroxyapatite particles were synthesized as a control for further identification and characterization. Hydroxyapatite was prepared by wet chemical precipitation method using calcite ( $\text{CaCO}_3$ ) and urea phosphate (UPH) as precursor materials. Specific amount of calcite as a source of calcium ions was added to 100 mL of deionized water followed by addition of UPH with respect to the Ca/P ratio of 1.67. Temperature was set at 50 °C and stirring was continued for 4 days. Obtained precipitate suspension was filtered, washed three times with deionized water and left to dry at room temperature. After drying, hydroxyapatite powder was obtained as a final product.

### ***2.4.4. In situ synthesis of composite hydrogels***

The preparation of the composite gelatin-tyramine/hydroxyapatite hydrogel was done by *in situ* wet precipitation method from previously mentioned calcium and phosphate precursors to obtain different hydroxyapatite content (2, 5 and 10%) in final composite. Starting 3% (w/v) polymer solution was prepared by dissolving gelatin-tyramine powder in deionized water. The pH of deionized water was previously adjusted at 7 by adding aqueous NaOH solution (1 mol/dm<sup>3</sup>). Then, specific amount of calcite was added into polymer solution with rigorous stirring at 37 °C. When homogeneous gelatin-tyramine/calcite suspension was achieved, specific amount of UPH with respect to the Ca/P ratio of 1.67 was added into the mixture. The reaction temperature was set at 50 °C and solution was stirred for 24 hours. The final suspension was cooled down to room temperature and subsequently frozen with liquid nitrogen, stored at -80 °C overnight and lyophilized.



As reference materials, gelatin-tyramine/hydroxyapatite composites were prepared by conventional mechanical mixing method as follows: hydroxyapatite particles, obtained by the synthesis method described in section 2.4.3., were added into 3 % gelatin-tyramine solution and rigorously stirred for 24 h at 50 °C. The final solution was cooled down to room temperature and subsequently frozen with liquid nitrogen, stored at -80 °C overnight and lyophilized.

#### ***2.4.5. Injectable composite hydrogel preparation***

The chemical crosslinking of gelatin-tyramine/hydroxyapatite composite was done by firstly preparing 3% composite solution from lyophilized sample obtained in section 2.4.4. The crosslinking reaction was achieved using 10% of the total hydrogel volume of 20 U/mL of HRP and 10% of the total hydrogel volume of 10 mmol/dm<sup>3</sup> H<sub>2</sub>O<sub>2</sub> solution. Then, the mixture was quickly stirred to obtain a homogeneous solution which allowed formation of a hydrogel at room temperature in few minutes. After crosslinking, the samples were washed with deionized water dried and stored for further characterization.

### ***2.5. Materials characterization***

#### ***2.5.1. The pH monitoring***

The pH of the prepared solutions was measured using Schott CG 842 pH-meter with BlueLine14 electrode. The pH was measured at each step of described syntheses.

#### ***2.5.2. Fourier transform infrared spectroscopy***

All prepared samples were characterized by Fourier transform infrared spectroscopic analysis (FTIR). FTIR spectra were recorded by ATR-FTIR Bruker Vertex 70 spectrometer with diamond crystal, 16 times in the absorption mode in the range of 4000 – 400 cm<sup>-1</sup> with a resolution of 4 cm<sup>-1</sup> at 20 °C.

### ***2.5.3. X-ray diffraction analysis***

Mineralogical composition of the dried hydrogels was determined by X-ray diffraction analysis (XRD) on a Shimadzu XRD 6000 instrument with Cu K $\alpha$  radiation at 40 kV and 30 mA. The measuring range of angles of  $5^\circ < 2\theta < 70^\circ$  with scan rate of 0.2°/s. Identification of crystal phase was carried out with ICDD database (The International Centre for Diffraction Data).

### ***2.5.4. Scanning electron microscopy***

The morphology of lyophilized hydrogels was investigated by scanning electron microscopy (SEM) on the instrument TESCAN Vega3SEM EasyProbe in electron beam energy of 10 kV. Prior to scanning, the samples were exposed to plasma of gold and palladium for 120 seconds.

### ***2.5.5. Equilibrium swelling***

The swelling capacity of prepared crosslinked hydrogels was evaluated in deionized water. Previously weighed samples were immersed in deionized water for 2 h at room temperature (no longer times were measured to avoid hydroxyapatite dissolution from the samples). The swollen hydrogels were removed from the medium and the remained water excess was absorbed with a filter paper. As such, samples were weighed with a microbalance. The equilibrium swelling ratio (ESR) was calculated using the following equation 1:

$$\text{ESR} = (m_s - m_d)/m_d \quad (1)$$

Where  $m_s$  and  $m_d$  are the mass of the hydrogels at the swollen state and at the dry state, respectively.

## **2.6. Rheological properties**

Rheological characterization of prepared hydrogels was carried out by a Discovery HR-2 Hybrid Rheometer (TA Instruments) using a cone and plate geometry of 20 cm diameter. The gap between the upper and lower plates was kept at of 900  $\mu\text{m}$ . The measurements were taken at 25 °C using solvent trap to create a thermally stable vapour barrier, virtually eliminating any solvent loss during the experiment.

The influence of the time ( $t_s$ ), the shear strain ( $\gamma$ ) and the angular frequency ( $\omega$ ) on shear storage modulus ( $G'$ ) and loss modulus ( $G''$ ) of hydrogel was measured.

The time dependence of the shear storage and loss modulus was examined on the *in situ* gelation of the hydrogel in the shear deformation of 2% and the frequency of 0.2 Hz.

The strain amplitude of crosslinked hydrogel was verified in the range of 0.01 to 100 % of deformation at 0.2 Hz to ensure linear viscoelastic region of hydrogel, where storage modulus ( $G'$ ) and loss modulus ( $G''$ ) are independent of the strain amplitude.

Finally, dynamic frequency sweep tests of crosslinked hydrogels were performed in order to determine the dependence of storage and loss modulus on frequency ( $100 < \omega < 0.01$  Hz) at constant strain corresponding to the linear viscoelastic region of the hydrogel.

### 3. Results and discussion

#### 3.1. FTIR identification

The FTIR spectra of identification of prepared hydroxyapatite particles and composite hydrogels by infrared spectroscopy are given in figures 4 – 6. The FTIR identification of all prepared systems is focused on wave number range of 4000 – 400  $\text{cm}^{-1}$  to characterize calcium phosphate phase formed by *in situ* precipitation reactions.

Figure 4 shows spectrum of hydroxyapatite particles as a control sample for identification of further *in situ* formation of apatite phase within the gelatin-tyramine matrix, with its characteristic bands: the band at 1026  $\text{cm}^{-1}$  corresponds to the asymmetric stretching of the phosphate ( $\text{PO}_4^{3-}$ ) bonds, while absorption band at 962  $\text{cm}^{-1}$  corresponds to the symmetric stretching of the  $\text{PO}_4^{3-}$  bonds. Besides stretching, the asymmetric bending of phosphates was observed at 561  $\text{cm}^{-1}$  [37]. These are the most characteristic chemical groups in the FTIR spectrum of synthesized hydroxyapatite. [38].

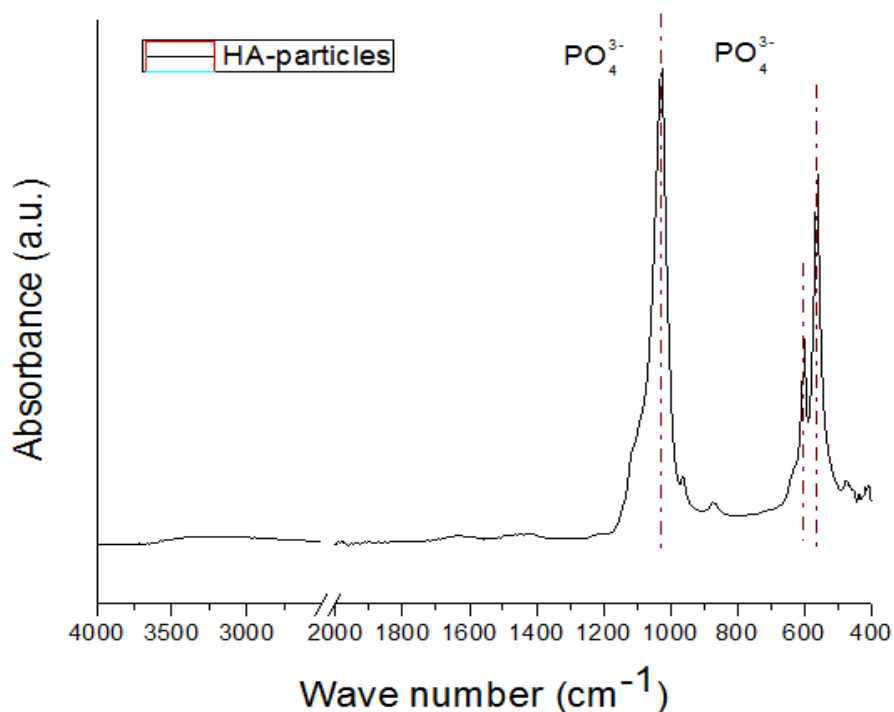


Figure 4. FTIR spectrum of hydroxyapatite particles.

Beside characteristic phosphate bands, weak absorption bands at wave number of 1454 and 1421  $\text{cm}^{-1}$  are associated with carbonate groups ( $\text{CO}_3^{2-}$ ). The presence of  $\text{CO}_3^{2-}$  bands can signify substitution of phosphate ions, which means formation of a B-type substituted hydroxyapatite [39-40].

The figure 5 illustrates the FTIR spectra of injectable composite hydrogels with different content of *in situ* formed hydroxyapatite compared with pure gel-tyramine hydrogel. All prepared hydrogels show absorption bands at 561  $\text{cm}^{-1}$  and 601  $\text{cm}^{-1}$  associated with the asymmetric bending of  $\text{PO}_4^{3-}$  bond, and band at 1035  $\text{cm}^{-1}$  confirming formation of apatite phase [39]. The clarity of phosphate band increases by the concentration of hydroxyapatite precursors, with most observable intensity in composite with 10% of HA.

The amine absorption band arising from N-H stretching of gelatin-tyramine matrix was distributed at 3270 – 3370  $\text{cm}^{-1}$ , while C-H stretching is observed by the band at 2947  $\text{cm}^{-1}$ . Characteristic amid bands were found at 1633  $\text{cm}^{-1}$  for the carbonyl group in amid bond (amid I), while N-H deformation at 1540  $\text{cm}^{-1}$  (amid II) [40]. The band at 1429  $\text{cm}^{-1}$  corresponds to C=O asymmetric stretching vibration [41]. Since gelatin-tyramine possesses strong intensity through all measured region, identification of carbonate groups substituted in hydroxyapatite lattice is very difficult.

It is assumed that, during the *in situ* apatite reactions within gelatin-tyramine matrix, the calcium ( $\text{Ca}^{2+}$ ) ions from hydroxyapatite precursors (calcite) can form specific complexation with carboxyl ( $-\text{COO}^-$ ) ions of gelatin molecules allowing nucleation sites for apatite crystal formation [42].

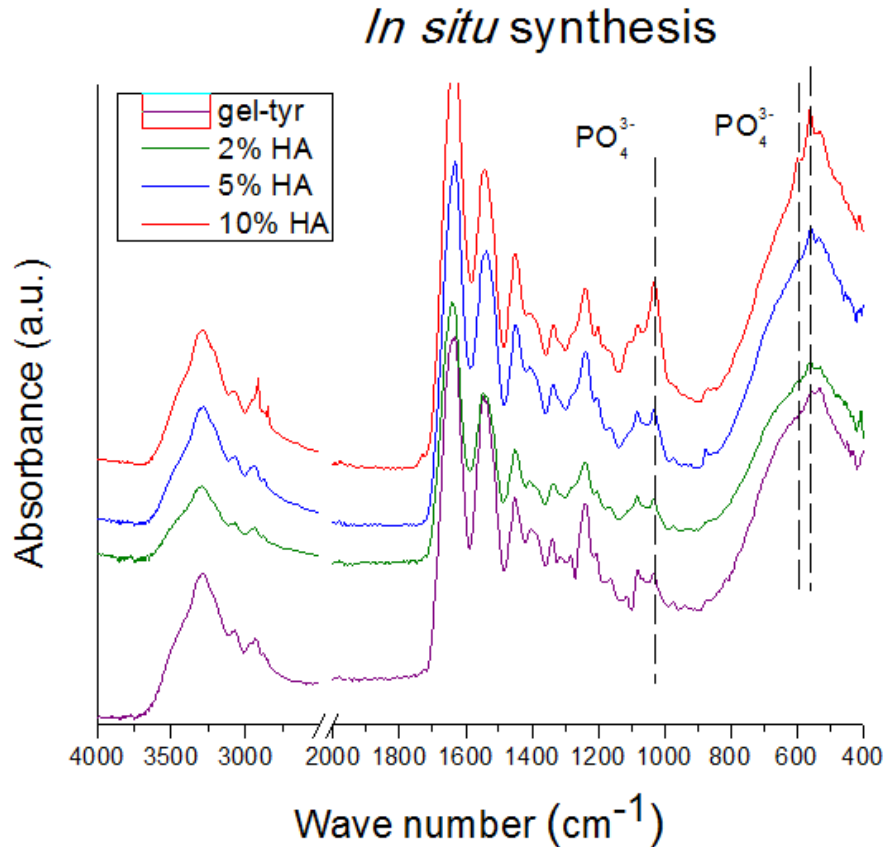


Figure 5. FTIR spectra of gelatin-tyramine/*in situ* HA hydrogels.

The FTIR spectra of control materials obtained by conventional mechanical mixing of hydroxyapatite particles within gelatin-tyramine matrix are shown in figure 6. As it can be seen, control materials show very similar spectra as hydrogels prepared by *in situ* synthesis. The characteristic bands for phosphate group indicating the presence of apatite phase in composite hydrogels can be found at 1033, 601 and 561  $\text{cm}^{-1}$ . Once again, characteristic amid bands of gelatin-tyramine are noted at 1633 and 1544  $\text{cm}^{-1}$ .

The significant difference in absorption spectra of *in situ* formed composites and control materials has not been observed, from which successful *in situ* apatite formation can be confirmed.

## Mechanical mixing

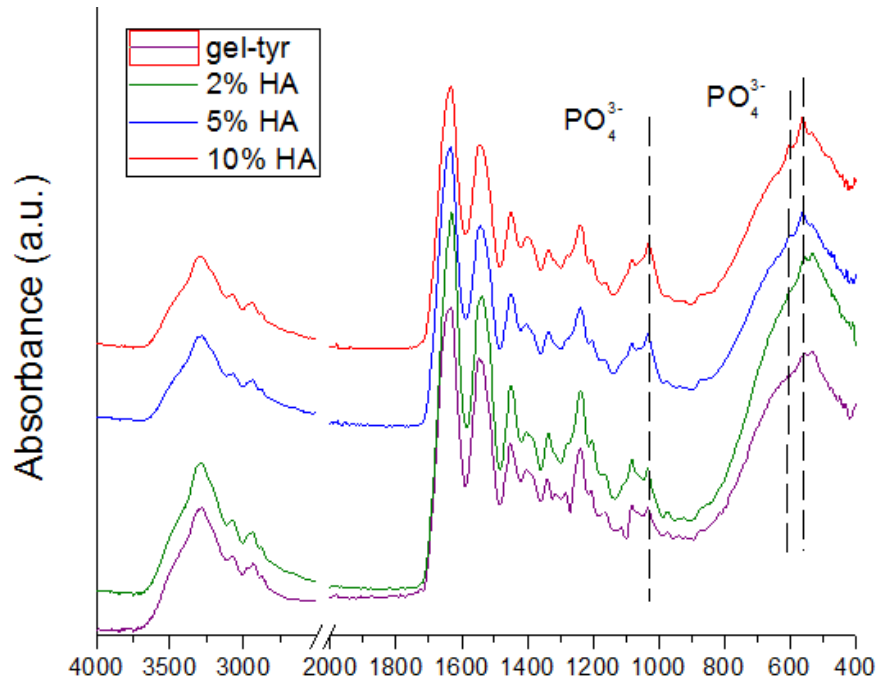


Figure 6. FTIR spectra of gelatin-tyramine/HA particles hydrogels.

### ***3.2. Determination of mineralogical composition***

The mineralogical composition of synthesized hydroxyapatite particles was confirmed by X-ray powder diffraction analysis (XRD) and ICDD (International Centre for Diffraction Data) card catalogue. The XRD patterns of hydroxyapatite particles and hydroxyapatite standard (ICDD 9-432) are given in figure 7.

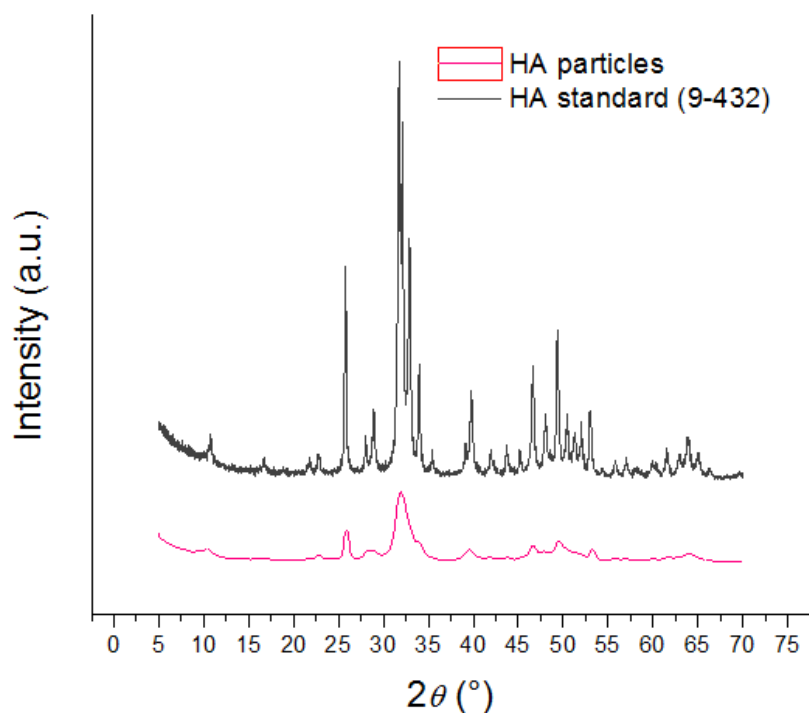


Figure 7. XRD patterns of hydroxyapatite particles and hydroxyapatite standard (ICDD 9-432).

Comparing the obtained pattern, hydroxyapatite as the only mineralogical phase of synthesized particles has been observed. Regarding the morphology of the particles, low crystallinity associated with small crystals can be indicated by wider X-ray diffraction maxima at  $2\theta = 26^\circ$  and  $32^\circ$ .

XRD diffraction patterns of *in situ* formed composite hydrogel are shown in figure 8. The presence of gelatin in composite hydrogels is identified with typical maxima at  $2\theta = 7.8^\circ$  ( $d_{101} = 11.08 \text{ \AA}$ ) and at  $22.12^\circ$  ( $d_{101} = 4.01 \text{ \AA}$ ), as shown in figure 8. These characteristic diffraction maxima are usually assigned to the triple-helical crystalline structure in collagen and gelatin.

The apatite phase is confirmed by the maximum at  $2\theta = 32^\circ$  clearly visible for composite hydrogel consisted of 10 % of hydroxyapatite. A broad maximum indicates low crystallinity of *in situ* formed apatite, which can be accompanied by better dispersion of inorganic phase within gelatin-tyramine matrix. Such crystallographic structure resembles the morphology of the



biological apatite of natural bone and has a larger specific surface area. Low intensity of characteristic hydroxyapatite maximum in other composite hydrogels (2% HA and 5% HA) could be due to lower precursors fraction. The XRD patterns indicate that hydroxyapatite is only inorganic phase, while traces of other calcium phosphates were not detected by this technique.

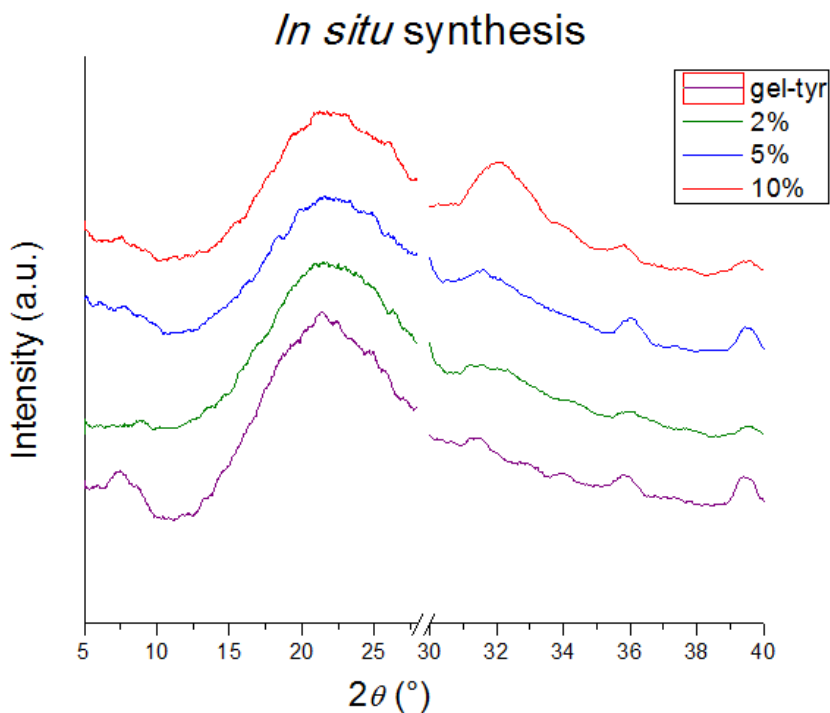


Figure 8. XRD patterns of gelatin-tyramine/*in situ* HA hydrogels.

The control samples of composite hydrogels show similar X-ray diffraction patterns regarding the *in situ* synthesized ones (figure 9). The notable difference in the shape of diffraction maximum at  $2\theta = 32^\circ$  is observed for composite with 10% of HA particles as more narrow with respect to the composite with 10% of *in situ* HA. This effect could indicate greater crystallinity of HA particles which are added into gelatin-tyramine matrix. Moreover, composite hydrogel with 5% of HA particles shows clearer diffraction maximum at  $2\theta = 32^\circ$  which could also be a result of possible particle agglomeration into bigger grains during mechanical mixing.

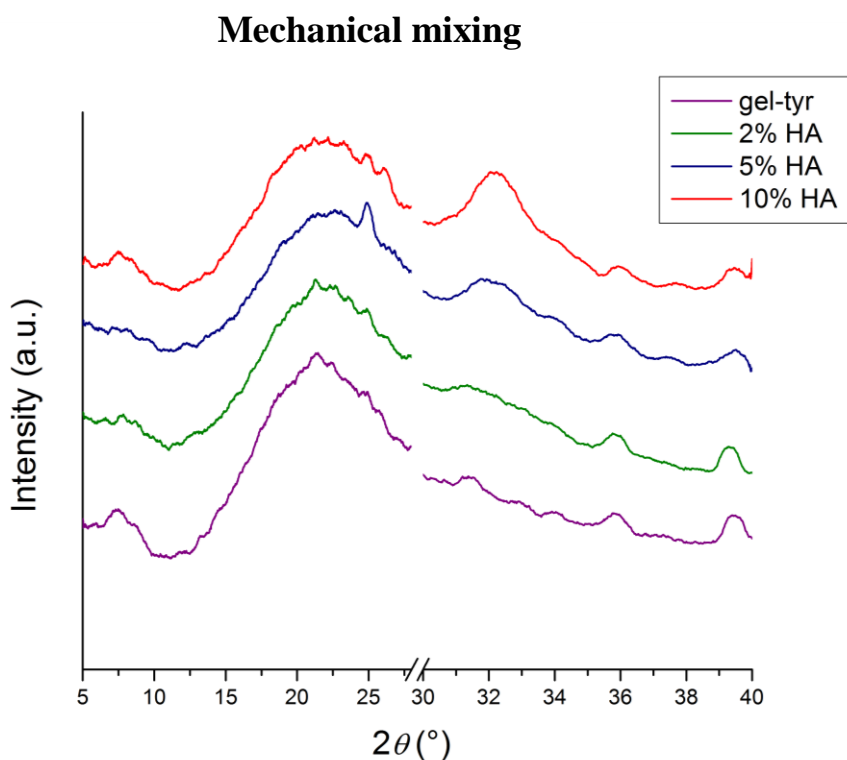


Figure 9. XRD patterns of gelatin-tyramine/HA particles hydrogels.

### 3.3. Microstructure of injectable hydrogels

Since the morphology of a hydrogel contributes significantly to its ability to encapsulate cells, the morphology of the surface and cross section has been examined by SEM imaging. Figure 10 shows SEM micrographs of the pure gelatin-tyramine, *in situ* synthesized composite hydrogels and control materials. Prior to imaging, all samples were shock-frozen in liquid nitrogen, quickly transferred to a freeze drier and lyophilized for 72 h. The lyophilization procedure is used to preserve the porous microstructure of prepared hydrogels by withdrawing the water through sublimation under vacuum, after having the product frozen: by heating up water in a frozen state under very low air pressure conditions, the water changes directly into the gaseous state (steam). This released steam is caught up in a cooling coil and removed. This technology allows keeping the quality of the product unchanged. This is the only way of drying, which does not change the molecular structure of the various molecules of the product [41].

Comparing the hydrogel micrographs, changes in the microstructure of the composite material are visible by increasing the fraction of hydroxyapatite. The presence of apatite agglomeration can be seen at higher HA content as a result of stronger interactions between HA phase.

The *in situ* synthesis of composite hydrogels resulted with formation of smaller plate-like hydroxyapatite crystals resembling the biological bone tissue. Additionally, those crystal show typical cauliflower morphology already reported by other studies [37, 43].

In contrast to the *in situ* formed composites, control materials have shown irregular particles of hydroxyapatite agglomerated in larger clusters, which is clearly visible in control sample with 10% of HA particles (figure 10g). This could be an effect of poor particle distribution which leads to precipitation of inorganic phase and non-homogeneity of the hydrogel.

Based on SEM imaging, *in situ* synthesis of gelatin-tyramine/hydroxyapatite composite has allowed formation of smaller apatite crystals ensuring higher specific area of osteoinductive component.

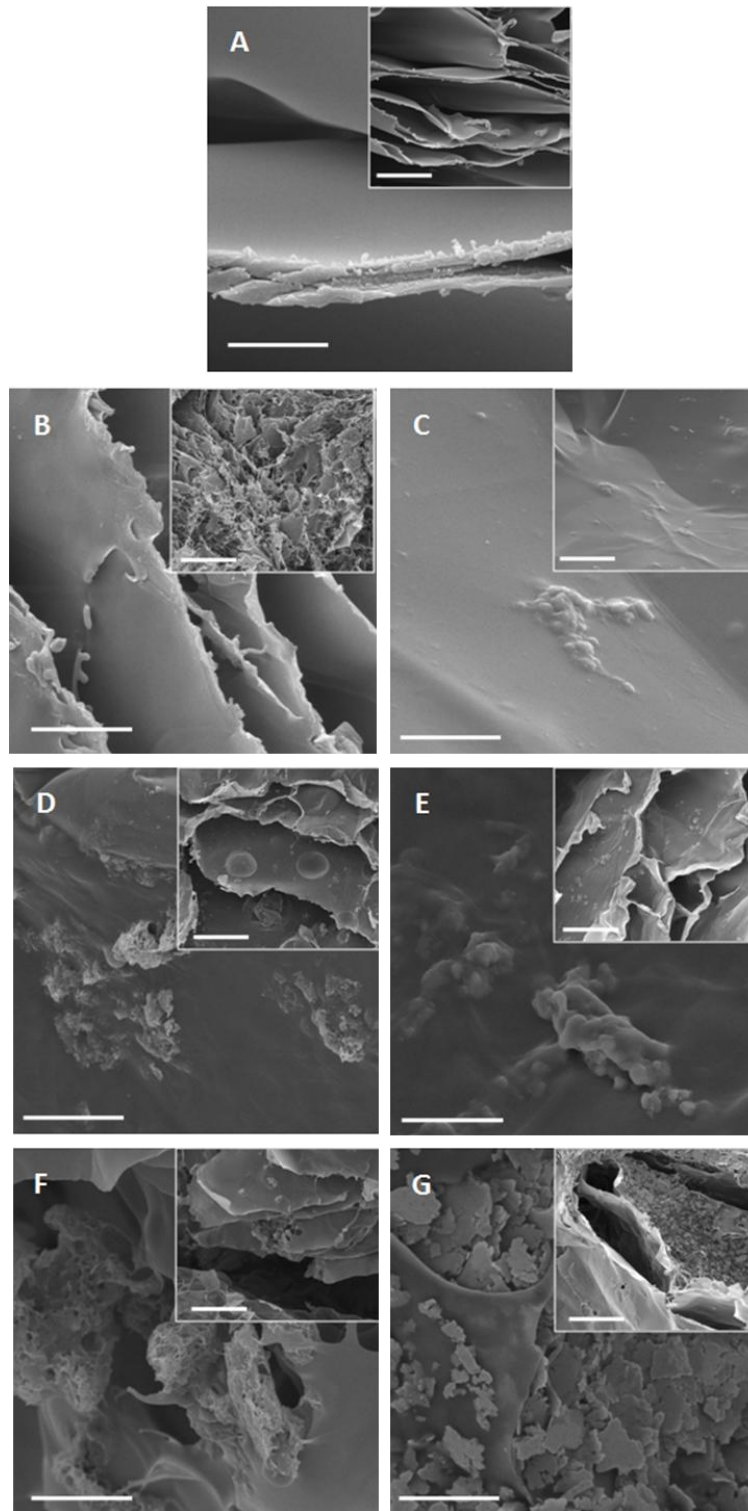


Figure 10. SEM images of composite hydrogels: A) gelatin-tyramine; B) 2% *in situ* HA; D) 5% *in situ* HA; F) 10% *in situ* HA; C) 2% HA particles; E) 5 % HA particles; and G) 10% HA particles.

Scale bar: 10 and 50  $\mu\text{m}$ .

### 3.4. Equilibrium water swelling of crosslinked hydrogels

One of the main factors that influence the diffusion of nutrients and the mechanical properties of hydrogels is the swelling property, which is related to the porosity of the systems and crosslinking degree. All prepared hydrogels show high swelling ratio with values higher than 2500 % after 2 h being immersed in water (figure 11), which is of great importance for cells and nutrients diffusion. The equilibrium water content indicates that hydrogels have capacity to uptake and retain water content greater than their own weight which is advantage in practical applications to have stable implant during cell culture or implanted site contact.

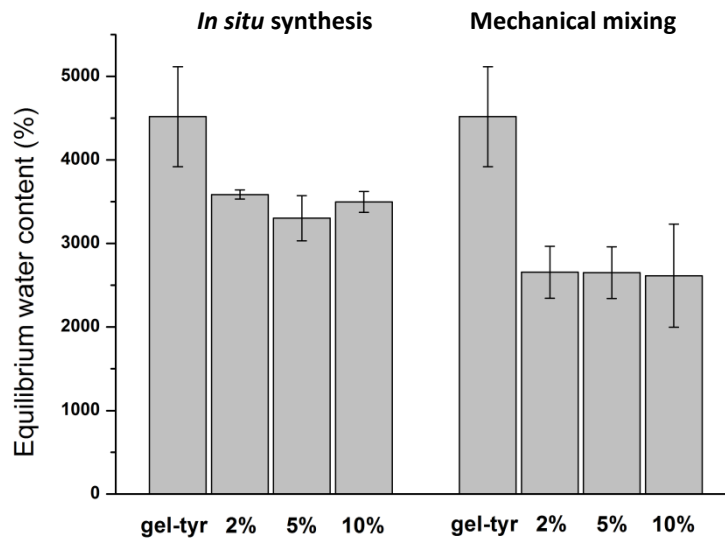


Figure 11. Swelling capacity of crosslinked injectable hydrogels.

As seen from figure 11, the presence of hydroxyapatite influences the content of absorbed water causing constrain during the swelling. This effect can be described as a formation of HA barrier that prevents water permeation into gelatin-tyramine matrix. The significant difference in swelling capacity of *in situ* formed composite hydrogels has not been observed, although, *in situ* synthesis have provide higher swelling of hydrogels with respect to the control materials. This could be a result of better matrix-filler interactions and lower interface energy without forming agglomerates. It seems that smaller crystals obtained by complex *in situ* hydroxyapatite formation, indicated by SEM analysis, stabilize the hydrocolloid structure of gelatin-tyramine during the swelling allowing greater water absorption.

### 3.5. Rheological properties of hydrogels

The hydrogel as an injectable system should have an optimum viscosity to allow secure coverage of the defect during the implantation without flowing down [44]. To improve knowledge regarding the gelation kinetics and gel mechanical properties, the rheological behaviour, decomposed in both components  $G'$  and  $G''$  modulus, has been monitored. Although the gelation time determination strategy, based on the intersection of elastic and viscous moduli, has been repeatedly used in literature, it often provides a rough approximation [45].

#### 3.5.1. Determination of gelation time

The gelation time of the composite hydrogels (table 2 and 3) were assessed by rheological testing using the time sweep test at 25 °C. The gelling time values of composite hydrogels and control materials crosslinked with HRP and H<sub>2</sub>O<sub>2</sub>, given in table 2 and 3, were determined as an intercept of tangents drawn at the beginning and the end of gelation curve (figure 12a). The gelation of *in situ* formed hydrogels shows high dissipation of values, in which significant difference is noted only for 10% of *in situ* HA. This behaviour can be related to viscosity increment due to larger apatite crystals formed by higher fraction of HA precursors. Nevertheless, possible experimental error due to difficult handle of the samples is also assumed.

Table 2. Gelation time of *in situ* formed composite hydrogels.

System	gel-tyr	2%	5%	10%
Gelation time (s)	205.68 ± 2.16	240.75 ± 43,42	203.8 ± 1.96	275.77 ± 2.93

Table 3. Gelation time of control materials.

System	gel-tyr	2%	5%	10%
Gelation time (s)	205.86 ± 2.16	229.79 ± 6.12	224.67 ± 1.78	227.83 ± 13.45

The control composite materials show similar gelation time regarding the different fraction of hydroxyapatite particles with respect to the pure gelatin-tyramine matrix. Taking into account

possible experimental errors, we can assume that hydroxyapatite presence does not influence the gelation time of crosslinked gelatin-tyramine hydrogel.

Regarding the shear strength during the crosslinking reaction, all investigated hydrogels show similar behaviour of storage modulus with time as rapid increment during the initial 200 s of testing followed by reaching the plateau which indicates completed crosslinking reaction.

### ***3.5.2. Shear strength of crosslinked composite hydrogels***

Figure 12a shows the typical time sweep profiles of shear behaviour for pure gelatin-tyramine, *in situ* formed composite hydrogels and control materials crosslinked with HRP and H<sub>2</sub>O<sub>2</sub>. To evaluate storage ( $G'$ ) and loss ( $G''$ ) modulus of each material, samples were subjected to oscillatory stress sweep experiment. This way, we applied shear stress range over which storage modulus is independent of the applied shear stress, defined as linear viscoelastic region (LVR). The LVR profiles of all crosslinked hydrogels are depicted in figure 12b, while shear parameters determined at 1 Hz and 25 °C are summarized in tables 4 and 5.

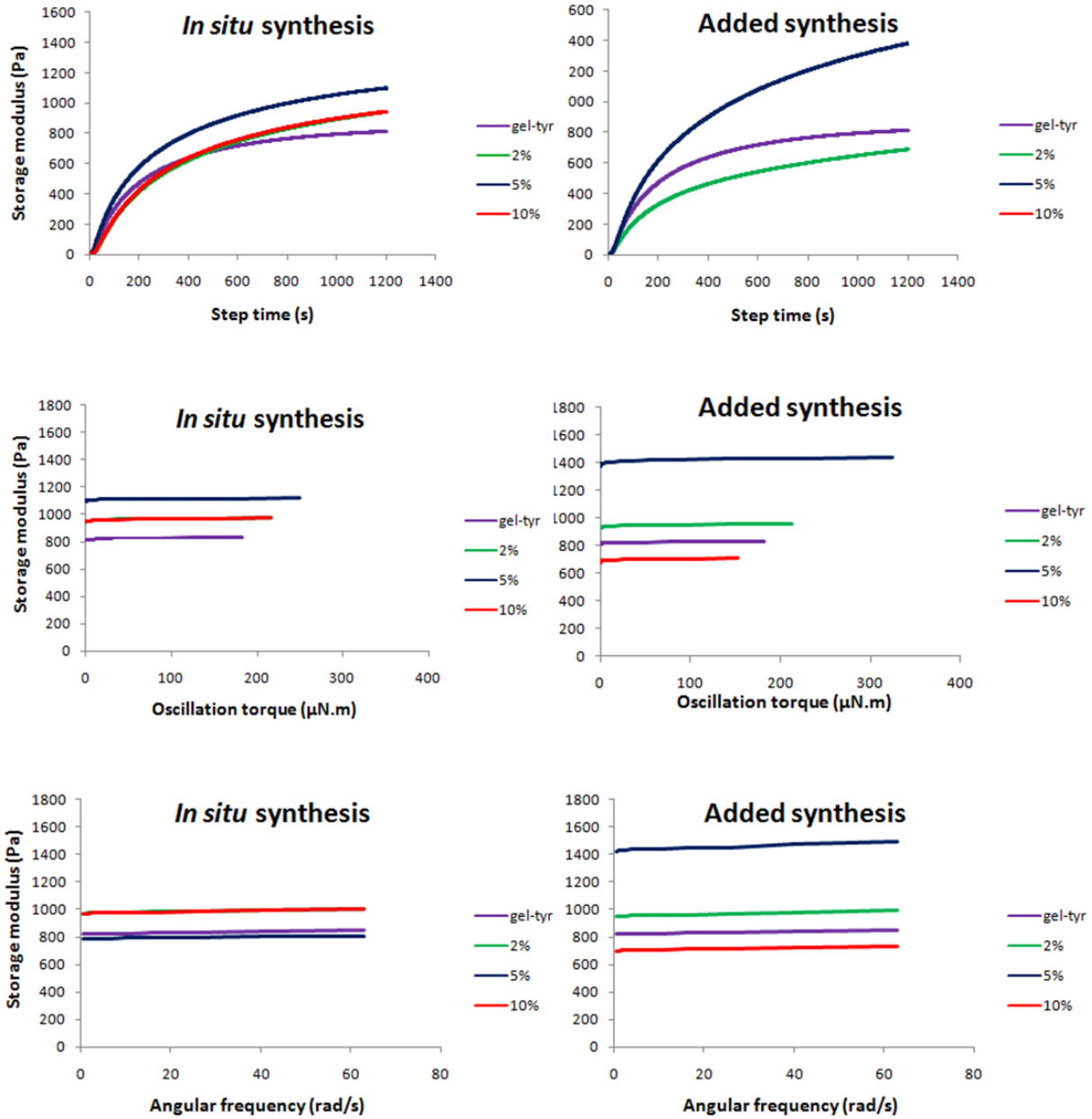


Figure 12. Rheological testing a) time sweep; b) oscillatory stress sweep; and c) oscillatory frequency sweep of composite hydrogels.

According to the strain amplitude testing, the presence of *in situ* hydroxyapatite show slight increment in shear strength of composite hydrogels regarding the pure gelatin-tyramine. It is possible that *in situ* HA synthesis has provided secondary interactions between polymer and filler resulting in higher persistence to shear deformation. However, significant influence of *in situ* HA fraction has not been observed.



Table 4. The shear parameters of *in situ* formed composite hydrogels determined at constant deformation of 1% and frequency of at 1 Hz.

	Storage modulus (Pa)	Loss modulus (Pa)	$\tan(\delta) \cdot 10^3$
gel-tyr	821.78 ± 39.39	1.21 ± 0.05	2.07 ± 1.12
2% HA	971.05 ± 76.94	1.98 ± 0.94	2.07 ± 1.12
5% HA	1119.67 ± 54.49	2.63 ± 0.48	2.92 ± 0.01
10% HA	1009.98 ± 45.58	1.18 ± 0.82	2.13 ± 1.01

Table 5. The shear parameters of control materials determined at constant deformation of 1% and frequency of at 1 Hz.

	Storage modulus (Pa)	Loss modulus (Pa)	$\tan(\delta) \cdot 10^3$
gel-tyr	821.78 ± 39.39	1.21 ± 0.05	2.07 ± 1.12
2% HA	949,14 ± 111.79	1.46 ± 0.10	2.20 ± 1.35
5% HA	1503.94 ± 73.22	1.79 ± 0.04	1.52 ± 0.15
10% HA	699.83 ± 293.10	0.88 ± 0.11	3.40 ± 0.58

During the evaluation of control materials, composite with 5% of HA particles has emerged as a sample with highest storage modulus, while sample with 10% has shown large values dissipation. Once again, a possible error cannot be neglected and re-evaluation of rheological behaviour of crosslinked hydrogels is required.

Finally, frequency sweep experiments (Figure 12 c) were carried out to investigate the gel properties of the cured systems, namely, the stability of three-dimensional crosslinked networks. The obtained data revealed that all hydrogels exhibit a plateau of storage modulus in wide range of frequency, which indicates stable crosslinked network of all prepared hydrogels.

The behaviour of crosslinked hydrogels can be characterized by the ratio between the loss modulus and storage modulus ( $G''/G'$ ). This ratio is defined as the loss factor ( $\tan(\delta)$ ) and can be calculated by the equation 2:

$$G''/G' = \tan(\delta) \quad (2)$$

For the ratio  $G''/G' > 1$ , material behaves as a viscous liquid, while for  $G''/G' < 1$  material acts as an elastic solid. It has been considered, that lower ratio indicates elastic material or a gel with greater number of network junctions [43].

## 4. Conclusions

Gelatin and hydroxyapatite are most frequently used components for preparation of potential bone tissue grafts due to its biocompatibility, biodegradation and osteoinductivity. In this work, injectable composite hydrogels based on tyramine modified gelatine and *in situ* formed apatite have been prepared and characterized using FTIR analysis, X-ray diffraction, SEM imaging and rheological testing.

- *In situ* synthesis showed a positive effect on the formation of hydroxyapatite (HA) as the calcium phosphate phase in the gelatin-tyramine matrix.
- The broad maximum obtained by XRD analysis indicates low crystallinity of *in situ* formed apatite similar to biological apatite.
- All prepared hydrogels show high swelling ratio which is advantage in practical applications to have stable implant. The presence of hydroxyapatite influences the reduction of swelling. With respect to the control materials, *in situ* synthesis has provided higher swelling of composite hydrogels.
- Investigated composite hydrogels show similar behavior of storage modulus with time as rapid increment followed by reaching the plateau which indicates completed crosslinking reaction
- Samples with *in situ* hydroxyapatite show slight increment in shear strength of composite hydrogels regarding the pure gelatin-tyramine
- A storage modulus plateau in wide range of frequency of all prepared injectable hydrogels indicates stable crosslinked network.

Based on the presented research, prepared injectable hydrogels show good potential for further investigation of physical and biological properties and clarification of the hydroxyapatite influence of gelation mechanism and hydrogel's bioactivity and osteoinductivity.

## 5. Literature

1. M. Wang, Developing bioactive composite materials for tissue replacement, *Biomaterials* **24** (2003) 2133-2151.
2. B.M., Watson, T.N., Vo, P.S., Engel, A.G. Mikos, Biodegradable, in situ-forming cell-laden hydrogel composites of hydroxyapatite nanoparticles for bone regeneration, *Industrial & Engineering Chemistry Research* **54** (2015) 10206-10211.
3. M.V., Regi, D.A., Navarette, Hard Tissue Biomineralization: How nature works, *RSC Nanoscience & Nanotechnology* **39** (2015) 1-26
4. S. Pina, J.M., Oliveira, R.L., Reis, Natural-based nanocomposites for bone tissue engineering and regenerative medicine: a review, *Advanced Materials* **27** (2015) 1143-1169.
5. C. D., Moreira, S.M., Carvalho, H.S., Mansur, M.M., Pereira, Thermogelling chitosan–collagen–bioactive glass nanoparticle hybrids as potential injectable systems for tissue engineering, *Materials Science and Engineering C* **58** (2016) 1207-1216.
6. R. Yunus Basha, T.S., Sampath Kumar, M. Doble, Design of biocomposite materials for bone tissue regeneration, *Materials Science and Engineering C* **57** (2015) 452-463.
7. A. Kumar Nayak, Hydroxyapatite synthesis methodologies: an overview, *International Journal of ChemTech Research* **2** (2010) 903-907.
8. T. Petrovčić, A. Pilipović, Hidrogelovi, *Polimeri* **32** (2011) 31-33.
9. E.M., Ahmed, Hydrogel: preparation, characterization, and applications: a review, *Journal of Advanced Research* **6** (2015) 105-121.
10. J. Nourmohammadi, A. Ghaee, S.H., Liavali, Preparation and characterization of bioactive composite scaffolds from polycaprolactone nanofibers-chitosan-oxidized starch for bone regeneration, *Carbohydrate Polymers* **138** (2016) 172-179.
11. J. Zhu, R.E., Marchant, Design properties of hydrogel tissue-engineering scaffolds, *Expert Review of Medical Devices* **8** (2011) 607-626.
12. J. Maitra, V.K., Shukla, Cross-linking in hydrogels – a review, *American Journal of Polymer Science* **4** (2014) 25-31.

13. A.P., Mathew, K. Oksman, D. Pierron, M.F., Harnad, Crosslinked fibrous composites based on cellulose nanofibers and collagen with in situ pH induced fibrillation, *Cellulose* **19** (2012) 139-150.
14. H.M., Mousa, A.P., Tiwari, J. Kim, S.P., Adhikari, C.H., Park, C.H., Kim, A novel in situ deposition of hydroxyapatite nanoplates using anodization/hydrothermal process onto magnesium alloy surface towards third generation biomaterials **164** (2016) *Materials Letters* 144-147
15. S.K., Bhullar, N.L., Lalla, S. Ramkrishna, Smart Biomaterials, *Reviews on Advanced Materials Science* **40** (2015) 303-314
16. F. Lee, J.E., Chung, M. Kurisawa, An injectable hyaluronic acid–tyramine hydrogel system for protein delivery, *Journal of Controlled Release* **134** (2009) 186-193.
17. F. Li, Y. Liu, Y. Ding, Q. Xie, A new injectable in situ forming hydroxyapatite and thermosensitive chitosan gel promoted by Na<sub>2</sub>CO<sub>3</sub>, *Soft Matter* **10** (2014) 2292-2303.
18. S. Sakai, K. Hirose, K. Taguchi, Y. Ogushi, K. Kawakami, An injectable, *in situ* enzymatically gellable, gelatin derivative for drug, delivery and tissue engineering, *Biomaterials* **30** (2009) 3371-3377.
19. M.K., Nguyen, E. Alsberg, Bioactive factor delivery strategies from engineered polymer hydrogels for therapeutic medicine, *Progress in Polymer Science* **39** (2014) 1236-1265.
20. S.K.H., Gulrez, S. Al-Assaf, G. Phillip, Hydrogels: methods of preparation, characterisation and applications, in: *Progress in molecular and environmental bioengineering - from analysis and modelling to technology applications*, editor: Angelo Carpi, ISBN: 978-953-307-268-5, InTech (<http://www.intechopen.com/>)
21. S.R., Van Tomme, G. Storm, W.E., Hennink, *In situ* gelling hydrogels for pharmaceutical and biomedical applications, *International Journal of Pharmaceutics* **355** (2008) 1-18.
22. A. Morelli, M. Betti, D. Puppi, C. Bartoli, M. Gazzarri, F. Chiellini, Enzymatically crosslinked ulvan hydrogels as injectable systems for cell delivery, *Macromolecular Chemistry and Physics* **217** (2016) 581-590.
23. K. Xu, K. Narayanan, F. Lee, K.H., Bae, S. Gao, M. Kurisawa, Enzyme-mediated hyaluronic acid–tyramine hydrogels for the propagation of human embryonic stem cells in 3D, *Acta Biomaterialia* **24** (2015) 159-171.

24. L.S., Wang, F. Lee, J. Lim, C. Du, A.C. Wan, S.S. Lee, M. Kurisawa, Enzymatic conjugation of a bioactive peptide into an injectable hyaluronic acid–tyramine hydrogel system to promote the formation of functional vasculature, *Acta Biomaterialia* **10** (2014) 2539-2550.
25. R.N., Raja Mohd Hafidz, C.M., Yaakob, I. Amin, A. Noorfaizan, Chemical and functional properties of bovine and porcine skin gelatin, *International Food Research Journal* **18** (2011) 813-817.
26. M. Azami, M. Rabiee, F. Moztarzadeh, Glutaraldehyde Crosslinked gelatin/hydroxyapatite nanocomposite scaffold, engineered via compound techniques, *Polymer composites* **31** (2010) 2112-2120.
27. R. Kumar, A. Sivashanmugam, S. Iseki, K.P., Chennazhi, R. Jayakumar, Injectable chitin-poly( $\epsilon$ -caprolactone)/nanohydroxyapatite composite microgels prepared by simple regeneration technique for bone tissue engineering, *ACS Applied Materials Interfaces* **7** (2015) 9399-9409.
28. J. Becker, L. Lu, M.B., Runge, H. Zeng, M.J. Yaszemski, M. Dadsetan, Nanocomposite bone scaffolds based on biodegradable polymers and hydroxyapatite, *Journal of Biomedical Materials Research* **103** (2015) 2549-2557.
29. M.G., Rauchi, M. Alvarez-Perez, D. Giugliano, S. Zeppetelli, L. Ambrosio, Properties of carbon nanotube-dispersed Sr-hydroxyapatite injectable material for bone defects, *Regenerative Biomaterials* **3** (2016) 1-12.
30. T.P., Nguyen, B.H., Phuong Doan, D.V., Dang, C.K., Nguyen, N.Q., Tran, Enzyme-mediated in situ preparation of biocompatible hydrogel composites from chitosan derivate and biphasic calcium phosphate nanoparticles for bone regeneration, *Advances in Natural Sciences: Nanoscience and Nanotechnology* **5** (2014) 1-5.
31. M.S., AlHammad, Nanostructure hydroxyapatite based ceramics by sol gel method, *Journal of Alloys and Compounds* **661** (2016) 251-256.
32. J. Kolmasn, S. Krukowski, A. Laskus, M. Jurkitewicz, Synthetic hydroxyapatite in pharmaceutical applications, *Ceramics International* **42** (2016) 2472-2482.
33. A. Siddharthan, S.K., Seshadri, T.S., Sampath Kumar, Rapid synthesis of calcium deficient hydroxyapatite nanoparticles by microwave irradiation, *Trends in Biomaterials & Artificial Organs* **18** (2005) 110-113.

34. N. Monmaturapoj, Nano-size hydroxyapatite powders preparation by wet-chemical precipitation route, *Journal of Metals, Materials and Minerals* **18** (2008) 15-20.
35. A.B.H., Yoruc, Y. Koca, Double step stirring: A novel method for precipitation of nano-sized hydroxyapatite powder, *Digest Journal of Nanomaterials and Biostructures* **4** (2009) 73-81.
36. H. Peng, J. Wang, S. Lv, J.Wen, J. Chen, Synthesis and characterization of hydroxyapatite nanoparticles prepared by a high-gravity precipitation method, *Ceramics International* **41** (2015) 14340-14349.
37. A., Rogina, *in situ* sinteza hidroksiapatita u matrici biorazgradivih polimera, Doktorska disertacija, Zagreb, 2015.
38. M.S.M., Arsad, P.M., Lee, Synthesis and characterization of hydroxyapatite nanoparticles and  $\beta$ -TCP particles, 2011 2nd International Conference on Biotechnology and Food Science IPCBEE **7** (2011) 184-188.
39. L. Berzina-Cimdina, N. Borodajenko, Research of calcium phosphates using fourier transform infrared spectroscopy, in: *Infrared Spectroscopy - Materials Science, Engineering and Technology*, editor: Theophanides Theophile, ISBN: 978-953-51-0537-4, InTech (<http://www.intechopen.com/books/>).
40. M.J., Hossan, M.A. Gafur, M.R., Kadir, M.M., Karima Preparation and characterization of gelatin-hydroxyapatite composite for bone tissue engineering, *International Journal of Engineering & Technology* **14** (2014) 24-32.
41. H. Bundela, A.K., Bajpai, Designing of hydroxyapatite-gelatin based porous matrix as bone substitute: Correlation with biocompatibility aspects, *Express Polymer Letters* **2** (2008) 201-213.
42. <http://www.project-pharmaceutics.com/services/process-development> (13.08.2016)
43. A. Ressler, Razvoj biorazgradivih injekcijskih sustava na temelju kitozana i kalcijeva fosfata, Diplomski rad, Zagreb, 2016.
44. M. Mass, U. Hess, K. Rezwan, The contribution of rheology for designing hydroxyapatite biomaterials, *Current Opinion in Colloid & Interface Science* **19** (2014) 585-593.
45. M.J., Moura, M.M., Figueiredi, M.H. Gil, Rheological study of genipin cross-liked chitosan hydrogels, *Biomacromolecules* **8** (2007) 3823-3829.